The Polarity Protein Par6 Induces Cell Proliferation and Is Overexpressed in Breast Cancer

Marissa E. Nolan,[1,3] Victoria Aranda,[3] Sangjun Lee,[4] Balasubramanian Lakshmi,[3] Srinjan Basu,[2] D. Craig Allred,[4] and Senthil K. Muthuswamy[1,2,3]

[1]Graduate Program in Genetics, Stony Brook University, Stony Brook, New York; [2]Watson School of Biological Sciences, [3]Cold Spring Harbor Laboratory, Cold Spring Harbor, New York; and [4]Department of Pathology and Immunology, Washington University School of Medicine, St. Louis, Missouri

Abstract

The polarity protein complex Par6/atypical protein kinase (aPKC)/Cdc42 regulates polarization processes during epithelial morphogenesis, astrocyte migration, and axon specification. We, as well as others, have shown that this complex is also required for disruption of apical-basal polarity during the oncogene ErbB2-induced transformation and transforming growth factor β–induced epithelial-mesenchymal transition of mammary epithelial cells. Here, we report that expression of Par6 by itself in mammary epithelial cells induces epidermal growth factor–independent cell proliferation and development of hyperplastic three-dimensional acini without affecting apical-basal polarity. This is dependent on the ability of Par6 to interact with aPKC and Cdc42, but not Lgl and Par3, and its ability to promote sustained activation of MEK/ERK signaling. Down-regulation of Cdc42 or aPKC expression suppresses the ability of Par6 to induce proliferation, demonstrating that Par6 promotes cell proliferation by interacting with aPKC and Cdc42. We also show that Par6 is overexpressed in breast cancer–derived cell lines and in both precancerous breast lesions and advanced primary human breast cancers, suggesting that Par6 overexpression regulates tumor initiation and progression. Thus, in addition to regulating cell polarization processes, Par6 is an inducer of cell proliferation in breast epithelial cells. [Cancer Res 2008;68(20):8201–9]

Introduction

Par6 is a scaffolding molecule identified in *Caenorhabditis elegans* as a regulator of asymmetric cell division during embryonic development (1). In mammals, Par6 localizes to tight junctions (2, 3), axon tips (4), and nuclear speckles (5) and regulates diverse cellular processes. Par6 regulates establishment of apical-basal polarity (2, 3), inhibition of cell death (6), directional migration of astrocytes and keratinocytes (7, 8), and axon specification in neurons (4, 9). Thus, Par6 regulates diverse biological processes likely in a cell type–specific and context-specific manner.

Par6 is a scaffolding molecule that is involved in multiple protein-protein interactions (10, 11). The most prominent interactions are those made with the members of the Par polarity complex, which consists of Par3, an additional scaffolding molecule, atypical protein kinase (aPKC), and the GTP binding proteins Cdc42/Rac (12–15). These interactions are required for Par6 regulation of cell biological processes. For instance, Par6 regulates aPKC-induced phosphorylation of Lgl (16), Par1 (17), and Numb proteins (18) during establishment of apical-basal polarity in epithelial cells. Likewise, Par6-associated aPKC regulates glycogen synthase kinase 3β (GSK3β) activity to induce polarized migration of astrocytes (19) and promote cell death during three-dimensional epithelial morphogenesis (6). Thus, the Par6 complex can serve as a signaling node that regulates diverse biological processes by controlling activation of downstream pathways.

In addition to its role during normal cell biology, Par6 also regulates initiation and progression of cell transformation. For example, Par6 cooperates with Rac1/Cdc42 to transform fibroblasts (12). We recently found that Par6 interacts with the oncogene receptor tyrosine kinase ErbB2, and this interaction is required for ErbB2-induced disruption of cell polarity and inhibition of cell death in three-dimensional mammary epithelial structures (20). Par6 also cooperates with transforming growth factor β (TGFβ) receptor to promote TGFβ-induced epithelial-to-mesenchymal transition (21). Interestingly, among the three isoforms of Par6 (gene name *Pard6*), *Pard6a, Pard6b*, and *Pard6g*, the *Pard6b* isoform is located in a region of the genome that is frequently amplified and overexpressed in breast cancer (22–25). It is likely that Par6 not only cooperates with regulators of cell transformation but may also directly regulate cell transformation processes.

Here, we show that expression of Par6 induces epidermal growth factor (EGF)–independent proliferation of normal mammary epithelial cells by promoting activation of mitogen-activated protein kinase (MAPK) signaling. This function of Par6 was dependent on its ability to interact with aPKC/Cdc42, demonstrating that Par6 regulates cell proliferation pathways, in addition to its previously shown role as a regulator of cell polarity and cell migration. Furthermore, we show that Par6 is overexpressed both in human precancerous breast lesions and in estrogen receptor (ER)–positive breast cancers, suggesting that Par6 pathways are likely to play critical roles during initiation and progression of breast cancer. Thus, the polarity protein Par6 promotes transformation of epithelial cells not only by regulating cell polarity pathways but also by inducing cell proliferation.

Materials and Methods

Cell culture and stable cell line generation. MCF-10A cells were maintained, as previously described (26). Comma-1D β geo cells were kindly provided by Daniel Medina (Baylor College of Medicine) and maintained in DMEM/F12 supplemented with 2% fetal bovine serum (FBS), 10 μg/mL insulin, and 5 ng/mL EGF (27). HC11 cells were obtained from the Rosen laboratory and cultured according to Xian and colleagues (28). Preparation of virus and infection was performed as previously described (29). All cells lines were selected with 1 μg/mL of puromyocin.

Note: Supplementary data for this article are available at Cancer Research Online (http://cancerres.aacrjournals.org/).

Requests for reprints: Senthil K. Muthuswamy, One Bungtown Road, Cold Spring Harbor Laboratory, Cold Spring Harbor, NY 11724. Phone: 516-367-6975; Fax: 516-367-8461; E-mail: muthuswa@cshl.edu.

doi:10.1158/0008-5472.CAN-07-6567

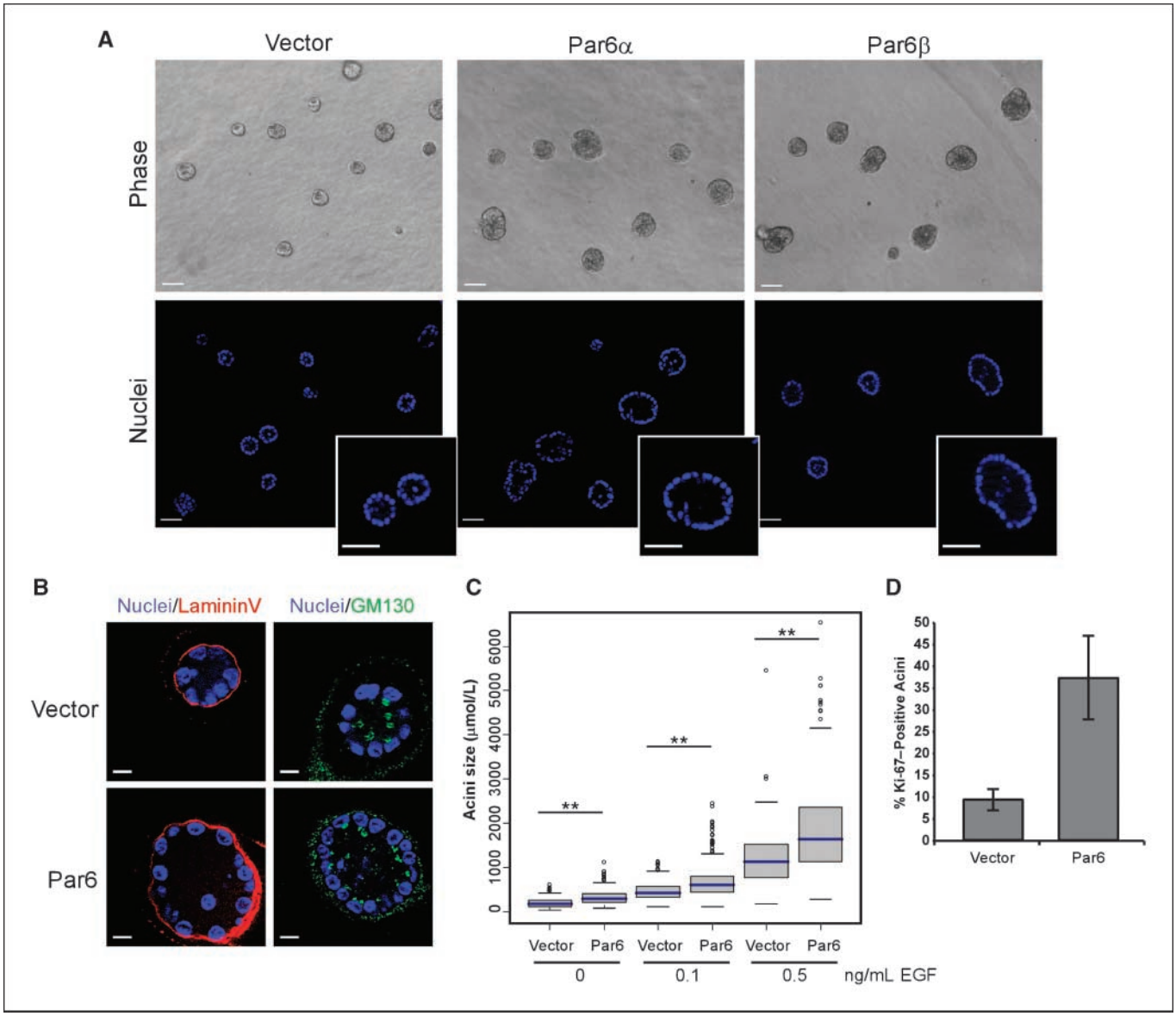

Figure 1. Overexpression of Par6 promotes proliferation without disrupting three-dimensional acini morphogenesis. *A,* phase contrast (*top*) and optical sections of acini stained with 4′,6-diamidino-2-phenylindole (DAPI; *bottom*). Images of day 20 acini grown in 0.5 ng/mL EGF; insets show detail of hollow lumen. *Scale bar,* 50 μm. *B,* immunofluorescence staining of day 12 acini structures grown in 0.5 ng/mL EGF with the apical marker GM130 (*green*) and basal marker Laminin V (*red*) and costained with DAPI to monitor nuclei. *Scale bar,* 10 μm. *C,* distribution of acini size (circumferential area) of day 12 acini structures grown in 0, 0.1, and 0.5 ng/mL EGF. Area of each acini was measured using Zeiss Axiovision 4.5 software and plotted as box plots. *Blue line,* median value; *spread,* 1.5 times the interquartile range; *circles,* outliers. Each condition represents ~800 acini structures from three dependent experiments. The *P* value between Vector and Par6 for each EGF concentration was <0.0001 calculated by Mann-Whitney test. *D,* quantitation of day 12 acini with at least one positive Ki-67–positive nuclei on day 12 acini structures grown in 0.5 ng/mL EGF. Data are represented as percentage of Ki-67-positive structures; *bars,* SD. Each bar represents ~700 acini from three independent experiments.

Cell growth and S-phase assays. MCF-10A (Vector, Par6α, K19A, ΔPro136, M235W, and Par6β) cells were grown to confluency under normal growth conditions and placed in assay medium (DMEM/F12 supplemented with 2% horse serum, 10 μg/mL insulin, 500 ng/mL hydrocortisone, and 100 ng/mL cholera toxin). Cells were then trypsinized, and 5×10^4 (growth curve) or 2.5×10^5 (S-phase) cells were plated in assay medium. For growth curve assays, cells were trypsinized and counted by hemacytometer on days 1, 3, 5, 7, 9, and 11. For S-phase assay, 30% of the assay media were changed on day 1, and cells were imaged by phase microscopy before harvesting on day 3. Cells were collected for flow cytometry by trypsinization and subsequent ethanol (70%) fixation. Cells were rehydrated in PBS with 1% calf serum and stained with 20 mg/mL propidium iodide (Sigma) containing 100 μg/mL RnaseA. Samples were analyzed using an LSRII flow cytometry (Becton Dickinson); at least 10,000 cells per sample were collected. Data from three independent experiments were analyzed using ModFit software (Verity). Comma-1D cells (Vector, Par6α) were grown to confluency under normal growth conditions and then placed in assay medium (DMEM/F12 supplemented with 0.5% FBS and 5 μg/mL insulin). 1×10^5 cells were plated, and cells numbers were counted on day 3 using a hemacytometer.

Three-dimensional morphogenesis assay. MCF-10A stable cell lines (Vector, Par6α, K19A, and Par6β) were trypsinized, and 4,000 single cells per well in an eight-well chamber slide (BD Biosciences) were coated with Matrigel. Cells were grown in assay medium with various amount of EGF (5, 0.5, 0.1, and 0 ng/mL). Medium was changed, and acini were imaged every 4 d. Day 12 acini structures were analyzed using AxioVison 4.5 (Zeiss). The acini size distribution of ~600 acini from three independent experiments was represented in a box plot. Each box represents 50% of the data within the interquartile range. The blue line

represents the median value, the spread represents 1.5 times the interquartile range, and outliers are shown as circles. Statistical analyses were performed using GraphPad Prism software and Mann-Whitney test. HC11 stable cell lines (Vector, Par6α) were grown on Matrigel with 0.5 ng/mL EGF, and day 12 structures were analyzed as done for MCF-10A cells.

Immunofluorescence. All immunofluorescence procedures were performed as previously described (26). Microscopy was performed on Zeiss Axiovert 200M using AxioVison 4.5 and ApoTome imaging system (Zeiss).

Biochemistry and immunoprecipitation. MCF-10A cells (Vector, Par6α, K19A, ΔPro136, M235W, and Par6β) were plated 2×10^6 in growth media, and cells were stimulated on day 5 with 2 μg/mL EGF. Cells were lysed in TNE buffer and immunoprecipitated with Flag or Par6 antibodies as described previously (20).

DNA constructs. Carboxy or amino-terminal Flagepitope tag mouse par6α was generated by PCR amplification of *mPar6α* from pFlag-CMV-mpar6α (14) and cloned into MSCV-PURO-IRES-GFP (kindly provided by S. Lowe, Cold Spring Harbor Laboratory). Point mutations of *mPar6α* were generated using site-directed mutagenesis. Amino-terminal Flag epitope-tag human Par6β was generated by PCR amplification from pBluescriptR-hPar6β (American Type Culture Collection) and cloned into MSCV-PURO-IRES-GFP. Two PCKι short hairpin vectors were obtained from Open Biosystems and subcloned into MSCV-LTR-PURO-IRES-GFP (30): targeting sequence for PKCι1 CACAGACAGTAA TTCCATATTAG and PKCι2 GATTATCTCTTCCAAGTTATTAG. Cdc42 short-hairpin vector number 3 was obtained from Open Biosystems and subcloned into MSCV-LTR-HYGRO-IRES-GFP (30). Cdc42 short-hairpin vector number 5 was generated by PCR and subcloned into MSCV-LTR-HYGRO-IRES-GFP: targeting

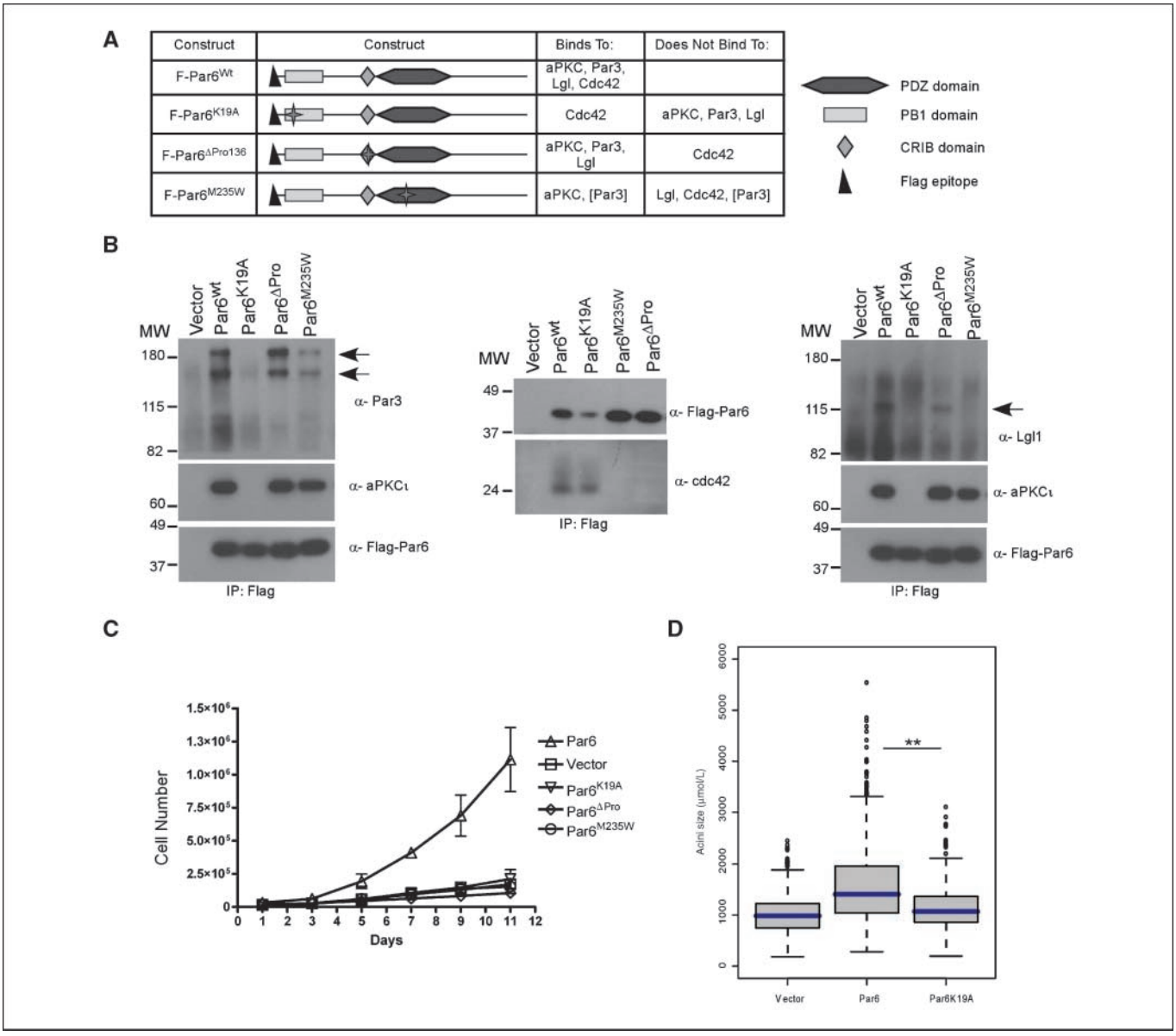

Figure 2. Par6-induced cell proliferation requires interaction with aPKC and Cdc42. *A,* table summary of the Par6 mutants and their different binding partners. *B,* immunoprecipitation of cell extracts with Par6 (anti-flag antibodies) and immunoblotting with anti-aPKCι, anti-Flag, anti-Par3, anti-Cdc42, and anti-Lgl antibodies. *C,* growth curve of vector control cells compared with $Par6^{wt}$ and mutant Par6 cells over a period of 11 d in EGF-free media. *Points,* means of estimated cell numbers from three independent experiments. *D,* distribution of acini size (circumferential area) of day 12 structures grown in 0.5 ng/mL EGF. Each condition represents ~800 acini structures from three dependent experiments. The *P* value between Vector and $Par6^{wt}$ or $Par6^{wt}$ and K19A is <0.0001 calculated by Mann-Whitney test.

sequence for Cdc42-3 CGGCCTAAAGAATGTATTTGAT and Cdc42-5 CAAGAATGTATTTGACGAAGCA.

Quantitative PCR. Twenty-five breast tumor samples were obtained from the Wigler laboratory (Cold Spring Harbor Laboratory). RNA was isolated using a Versagene RNA tissue kit (Gentra Systems). Normal breast tissue RNA was a gift from David Mu (Cold Spring Harbor Laboratory). Breast cancer cell line RNA was a gift from Adrian Krainer (Cold Spring Harbor Laboratory). MCF-10A control and Par6β-overexpressing RNA were obtained from trizol lysis (Invitrogen) according to the manufacturer's protocol. cDNA was generated using a Taqman reverse transcriptase kit (Roche). Quantitative real-time PCR was performed using SYBR green master mix (Applied Biosystems). The following primer sequences were used for Par6β, 5′-GTGAAGAGCAAGTTTGGAGC-3′ and 5′-GATGTCTGATAGCCTACCA-3′ and GAPHDH, 5′-CGACAGTCAGCCGCATCTT-3′ and 5′-CGTTGACTCCGA CCTTCA-3′. Samples were run on a Peltier thermalcycler (PTC-200) from MJ Research, and data were collected using an Opticon monitor chromo4 continuous fluorescence detector. Cycles were normalized to glyceraldehyde-3-phosphate dehydrogenase (GAPDH) and compared with MCF-10A or normal breast tissue Par6βlevels.

Antibodies. Antibodies used in this study were against Ki67 (Zymed); PKCι, GM130, Ccdc42, ERK2 (BD Biosciences); hPar6α antibody (previously described; ref. 20); mPar3 (Upstate Biotechnology); PKCζ (Santa Cruz Biotechnology); cleaved caspase-3, p-ERM, p-AKT (Cell Signaling Technology); Flag M2, β-actin (Sigma); laminin (Chemicon); p-ERK1 and p-ERK2, p-PKCι, Alexa-Fluor–conjugated secondary antibodies (Invitrogen).

Analysis of human breast cancers. Gene expression was performed on 112 breast tumors samples, and data were generously provided by Therese Sorlei and colleagues. The expression values are median-polished log ratios of expression in tumor cells to that in a reference cell mixture. A Kolmogorov-Smirnov null hypothesis test was used to calculate the *P* value.

Results

Overexpression of Par6 does not disrupt three-dimensional acini morphogenesis. Although *Pard6b* is amplified in breast cancer, it is not known what role, if any, overexpression of Par6 plays during transformation on breast epithelial cells. To investigate if overexpression of Par6 affects polarization and morphogenesis of mammary epithelial cells in three-dimensional culture, we expressed *Pard6a* (protein called Par6α) and *Pard6b* (protein called Par6β) in an EGF-dependent, nontransformed human mammary epithelial cell line, MCF-10A. When plated on Matrigel in the presence of EGF, MCF-10A cells form three-dimensional acini-like structures comprised of a single layer of polarized, proliferation-arrested epithelial cells surrounding a hollow central lumen (31). Overexpression of either Par6 isoform did not affect the ability of MCF-10A cells to form acini with hollow lumens (Fig. 1*A*). In addition, these acini had no detectable loss of apical-basal polarity as determined by using the apical polarity marker GM130, a basal polarity marker Laminin V (Fig. 1*B* and Supplementary Fig. S1), and a basolateral marker E-cadherin (data not shown). Thus, overexpression of Par6 did not affect polarization and morphogenesis of MCF-10A cells on Matrigel.

Overexpression of Par6 promotes cell proliferation. Although we did not detect any difference in the organization of the acinar structures, we did observe that Par6 expressing acini were larger than the control acini (Fig. 1*A*). To test the hypothesis that Par6 overexpression promotes acinar growth, acini size was quantitated by measuring the area occupied by each acinus. Par6α and Par6β overexpressing cells formed acini that were significantly larger than those formed by control cells, irrespective of the dose of EGF (Fig. 1*C* and Supplementary Fig. S2*B*). To determine if the increase in size was due to an increase in cell number or cell size, we counted the number of cells per structure. Acini derived from Par6-overexpressing cells had significantly more cells than those derived from control cells (Supplementary Fig. S3).

To determine if the increase in cell number is due to changes in cell proliferation rates, we monitored the presence of the proliferation marker Ki-67 during three-dimensional morphogenesis. Consistent with our previous results (31), acini derived from control cells had low proliferation rates on day 12 (Fig. 1*D*). However, acini derived from Par6-expressing cells had higher proliferation rates until day 20 compared with acini derived from control cells (Supplementary Fig. S4*A*). Furthermore, we did not observe any evidence for inhibition of cell death pathways in acini derived from Par6-overexpressing cells (Supplementary Fig. S4*B* and *C*). Thus, Par6 overexpression induces development of hyperplastic acini by inhibiting proliferation arrest during three-dimensional morphogenesis without disrupting polarity.

The ability of Par6 to promote proliferation was observed in multiple independent populations of MCF-10A cells and in a mouse mammary epithelial cell line, demonstrating that there was no clonal or cell line bias to the phenotype (Supplementary Fig. S5).

Par6-induced cell proliferation requires interaction with aPKC and Cdc42. To gain insight into the mechanisms by which Par6 induces cell proliferation, we generated Par6 mutants that are defective in binding to members of the Par6 complex, such as Par3, Cdc42, Lgl, and aPKC. We generated a lysine-to-alanine mutation in the PB1 (Phox/Bem1p) domain (K19A) to abolish binding to aPKC, deleted Proline 136 in the semi-CRIB binding domain (ΔPro136) to disrupt binding to Cdc42, and substituted a methionine with a tryptophan in the PDZ domain (M235W) to disrupt binding to Lgl (refs. 14, 32–35; Fig. 2*A*). Each mutant was expressed in MCF-10A cells, and the ability of the mutants to interact with components of the Par complex was determined by coimmunoprecipitation analysis (Fig. 2*B–D*). As expected, K19A failed to associate with aPKC and retained its ability to associate with Cdc42 (Fig. 2*B*). In addition, we found that this mutant also lost its ability to interact with Par3 and Lgl (Fig. 2*B*). The ΔPro136 mutant was defective in its ability to bind Cdc42 but associated with Par3, aPKC, and Lgl. The M235W mutant did not bind Cdc42, Lgl and was defective in binding Par3 but still associated with aPKC (Fig. 2*B*).

Stable populations of MCF-10A cells expressing comparable levels of the Par6 mutants were generated and analyzed for EGF-independent cell proliferation. None of the mutants induced EGF-independent cell proliferation in monolayer cultures (Fig. 2*C*) or enhanced cell proliferation during acini formation (Fig. 2*D* and data not shown). The inability of $Par6^{K19A}$ to promote proliferation showed that aPKC binding was necessary and that Cdc42 binding is not sufficient. Conversely, the $Par6\Delta^{Pro136}$ mutant showed that interaction with Cdc42 was necessary whereas aPKC, Par3, and Lgl were not sufficient to promote proliferation. The inability of $Par6^{M235W}$ to promote proliferation confirmed our conclusion that interaction with Cdc42 was necessary and that an interaction with aPKC was not sufficient to induce EGF-independent proliferation. Because the binding of Cdc42 to Par6 induces aPKC kinase activity in the Par6 complex (3, 7), it is likely that Par6-aPKC-Cdc42 forms a core complex to promote EGF-independent cell proliferation of mammary epithelial cells.

Par6-induced cell proliferation requires both aPKC and Cdc42. To determine if aPKC and Cdc42 play a role during Par6-induced cell proliferation, we knocked down expression of aPKC and Cdc42 in both control and Par6-expressing cell lines using two independent short hairpin RNAs for each aPKC and

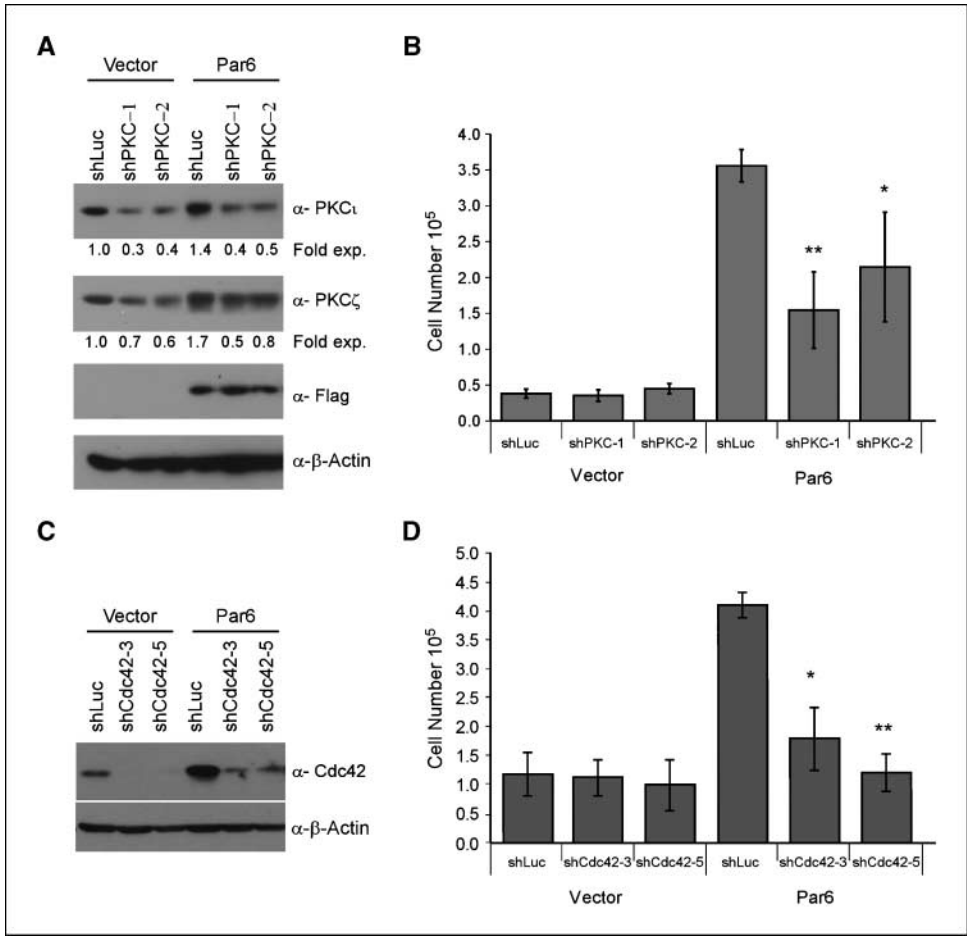

Figure 3. Par6-induced cell proliferation requires aPKC and Cdc42. *A,* cell extracts from PKC short hairpin–infected MCF-10A cells immunoblotted with indicated antibodies. The numbers below the bands refer to fold change in PKCι and PKCζ protein expression normalized to β-actin as determined by densometric analysis. *B,* the indicated cells were grown in EGF-free media for 7 d, and cell number was determined. *Columns,* means of quantitated cell numbers from three independent experiments; *bars,* SD. Student's *t* test was performed showing statistical significance between $Par6^{wt}$shLuc and $Par6^{wt}$shaPKC1 ($P = 0.004$) or $Par6^{wt}$shaPKC2 ($P = 0.04$). *C,* cell extracts from Cdc42 short hairpin–infected MCF-10A cells immunoblotted with indicated antibodies. *D,* the indicated cells were grown in EGF-free media for 7 d, and cell number was determined. *Columns,* mean of quantitated cell numbers from three independent experiments; *bars,* SD. Student's *t* test was performed showing statistical significance between $Par6^{wt}$shLuc and $Par6^{wt}$shCdc42-3 ($P = 0.009$) or $Par6^{wt}$Cdc42-5($P = 0.0005$).

Cdc42 (Fig. 3*A*). The aPKC RNA interference (RNAi) vectors significantly down-regulated the expression level of PKCι and had a modest effect on the levels of PKCζ (Fig. 3*A*). Decreased expression of PKCι significantly impaired the ability of Par6-overexpressing cells to proliferate in the absence of EGF while having no significant effect on the basal proliferation observed in vector control cells (Fig. 3*B*).

We identified two independent short hairpins that target Cdc42 (Fig. 3*C*). Both RNAi vectors significantly down-regulated Cdc42 in both control and Par6-overexpressing MCF-10A cells (Fig. 3*C*). As observed for aPKC, down-regulation of Cdc42 inhibited the ability of Par6 to induce proliferation in the absence of EGF, whereas loss of Cdc42 did not have a significant effect on the basal proliferation observed in vector control cells (Fig. 3*D*). Together, these data show that aPKC and Cdc42 play a critical role during Par6-induced proliferation in MCF-10A cells.

Par6 overexpression activates MAPK signaling. To understand how Par6 expression promotes cell proliferation, we tested if Par6 induced autocrine production of growth factors or juxtacrine activation of cell-cell signaling pathways. Conditioned media from Par6-expressing cells failed to promote proliferation of vector control MCF-10A cells (data not shown). In addition, coculturing experiments showed that Par6-expressing cells did not induce EGF-independent proliferation of control cells (data not shown). These observations suggest that Par6 promotes proliferation in a cell autonomous manner.

We therefore investigated cell autonomous mechanisms by which Par6 promotes cell proliferation. Activation of the EGF receptor (EGFR) pathway is an attractive possibility, because our data showed that Par6 induces EGF-independent proliferation of MCF-10A cells (Fig. 2*D* and Supplementary Figs. S2*C* and S5*A*). However, we did not observe EGF stimulation–independent phosphorylation of EGFR in Par6-overexpressing cells (data not shown), suggesting that Par6 overexpression does not directly induce EGFR phosphorylation. To determine if Par6 activates pathways downstream of EGFR, we investigated activation of PLCγ, phosphatidylinositol 3-kinase (PI3K), Ras/MAPK, and c-Jun NH_2 kinase (JNK), both in the presence and in the absence of EGF stimulation. Par6 overexpression had no effect on activation of PLCγ, PI3K, or JNK pathways, either in the presence or in the absence of EGF (Fig. 4*A* and data not shown). However, Par6-overexpressing cells had a significant increase in extracellular signal-regulated kinase (ERK) phosphorylation in the absence of EGF stimulation. In the presence of EGF stimulation, ERK phosphorylation returned to basal levels by 30 minutes in vector control cells, whereas in Par6-overexpressing cells, it was prolonged for 60 (Fig. 4*B*) and 120 minutes (Supplementary Fig. *S*2D). In contrast to Par6, the Par6 mutants neither induced phosphorylation of ERK in the absence of EGF nor promoted sustained ERK phosphorylation in the presence of EGF (Fig. 4*B* and Supplementary Fig. S6).

To confirm that the effect of Par6 on proliferation is directly due to its effect on ERK activation, we inhibited ERK activation using the MAPK/ERK kinase (MEK) kinase inhibitor U0126. Treatment of Par6-overexpressing cells with U0126 blocked both basal and EGF-induced sustained ERK phosphorylation (data not shown). In addition, the inhibitor also blocked EGF-independent cell proliferation (Fig. 4*D*), suggesting a role for MEK kinase in Par6-induced cell proliferation. Thus, we conclude that Par6 overexpression promotes EGF-independent cell proliferation by activating the MEK/ERK signaling pathway.

Pard6b is overexpressed in ER-positive human breast tumors. Next, we investigated if the genes encoding for the Par6 family of proteins (*Pard6)* are targeted for overexpression in breast cancer. Interestingly, *Pard6b* (Chr. 20q13.13), but not *Pard6a* (Chr. 16q22.1) or *Pard6g* (Chr. 18q23), is located in a region of the genome that is frequently amplified in breast cancer (22–25), and this amplification correlated with increased *Pard6b* gene expression (23, 24). To directly test if *Pard6b* is overexpressed in primary human breast cancers, we performed quantitative PCR analysis from 25 primary breast tumors, 2 normal breast tissue samples, 6 breast cancer cell lines, and MCF-10A cells. We found that 6 of 25 primary tumors and 2 of 6 breast cancer cells express mRNA at least 2-fold more than the levels observed in their respective controls (Fig. 5*A* and *B*). Thus, among the *Pard6* family members, *Pard6b* is genomically amplified and transcriptionally up-regulated in breast cancer.

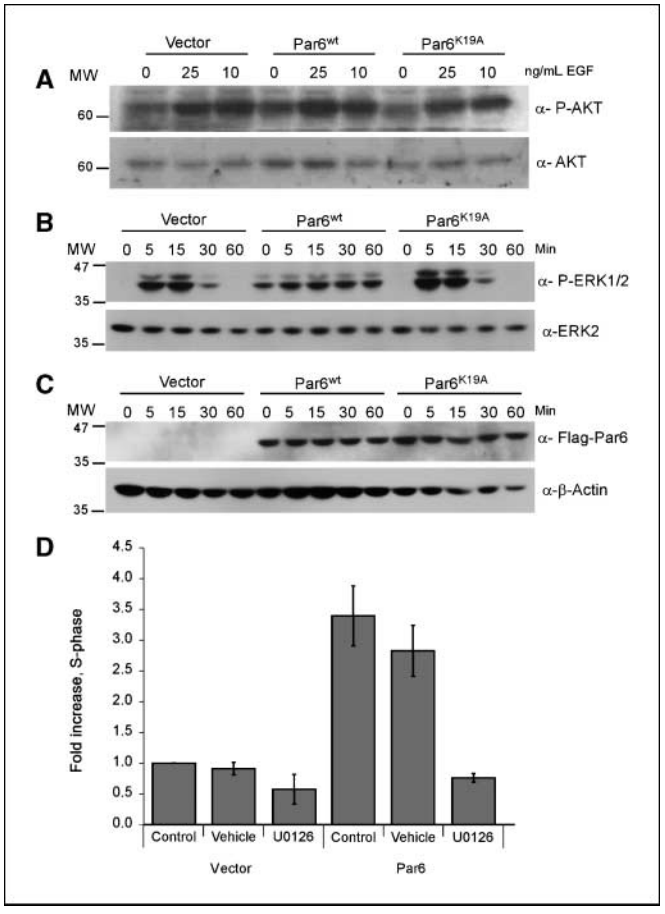

Figure 4. Par6 overexpression activates MAPK signaling. *A,* cell extracts from cells that were stimulated with 0, 10, and 25 ng/mL EGF for 15 min were immunoblotted with anti–phosphorylated-specific AKT and reprobed for total AKT. *B,* cell extracts from cells that were stimulated for 0, 5, 15, 30, and 60 min with 2 ng/mL EGF were immunoblotted with antibodies specific for phosphorylated ERK1/2 and reprobed with total ERK2. *C,* cell extracts were immunoblotted with anti-flag antibodies and reprobed with anti–β-actin. *D,* cells were grown in EGF-free media for 3 d with no inhibitors (Control), DMSO (vehicle), or MEK inhibitor (10 μmol/L UO126) and analyzed by flow cytometry. Data are fold increase in S-phase of Par6-expressing cells compared with control cells. *Columns,* means of three independent experiments; *bars,* SD.

Among the breast cancer cell lines tested, the two cell lines (MCF-7 and T47D) that overexpressed *Par6b* are also ER-positive, suggesting a relationship between *Par6b* overexpression and ER status. To determine if there is a relationship between ER status and *Pard6b* expression, we compared *Pard6b* mRNA levels in 68 of ER-positive and 44 of ER-negative breast tumors. Overexpression of *Pard6b* showed a significant positive correlation with ER+ status (Fig. 5*C*). We did not observe any relationship between Par6 overexpression and ErbB2 amplification in human breast tumors (data not shown), demonstrating that *Par6db* overexpression is specific to the ER-positive subtype of breast cancer. In addition, analysis of a public gene expression database Oncomine (36) showed that *Pard6b* expression positively correlated with ER in four independent studies (Supplementary Fig. S7; refs. 23, 37–39). Inhibition of ER signaling in MCF-7 cells by treatment with tamoxifen did not result in a significant decrease in the levels of *Par6db* mRNA (Supplementary Fig. S8), suggesting that *Pard6b* levels may not be directly regulated by estrogen. Thus, it is likely that overexpression of Par6 cooperates with EGF to provide a proliferative advantage to ER-positive breast cancers.

Almost all precancerous breast lesions are ER-positive (40). Furthermore, we recently showed that hyperplastic enlarged lobular units (HELU), the earliest histologically identifiable precursor of breast cancer, show high proliferation rates and an increased expression of members of both EGF and ER signaling modules (40, 41). Interestingly, like the three-dimensional acini derived from Par6 overexpressing MCF-10A cells, HELUs are hyperplastic structures wherein the acini are enlarged in size due to increase in cell number with no apparent loss of acinar architecture. Given the architectural similarity, we tested if Par6 was overexpressed in HELUs. RNA isolated from microdissected HELU and adjacent TDLU were analyzed by microarray (41). *Pard6b*, but not *Pard6a* or *Pard6g*, was overexpressed by 2.5-fold (P = 0.002) in HELUs compared with adjacent TDLUs. The gene encoding for PKCζ (*PRKCZ*), a component of Par6 complex, was also up-regulated by 1.46-fold (P = 0.029) compared with TDLUs (ref. 41; Fig. 5*D*). Thus, our results show that overexpression of Par6/aPKC is observed early in precancerous lesions and retained during development of ER-positive cancers.

It is possible that the Par6/aPKC/Cdc42 complex is a novel target for therapeutic intervention for both early and late stage of breast cancers. To test this possibility, we down-regulated expression of aPKC in a breast cancer–derived cell line, MCF7. Down-regulation of PKCι decreased cell proliferation (Fig. 6*A* and *B*), suggesting that inhibiting aPKC is likely to have important therapeutic relevance. Taken together, our results show that Par6/Cdc42/aPKC is a regulator of cell proliferation and suggests that the Par6 complex is a novel therapeutic target for breast cancer.

Discussion

We show that overexpression of Par6 in mammary epithelial cells promotes activation of MAPK and induces cell proliferation. In addition, we show that Par6 is overexpressed in both precancerous human breast lesions and in advanced breast

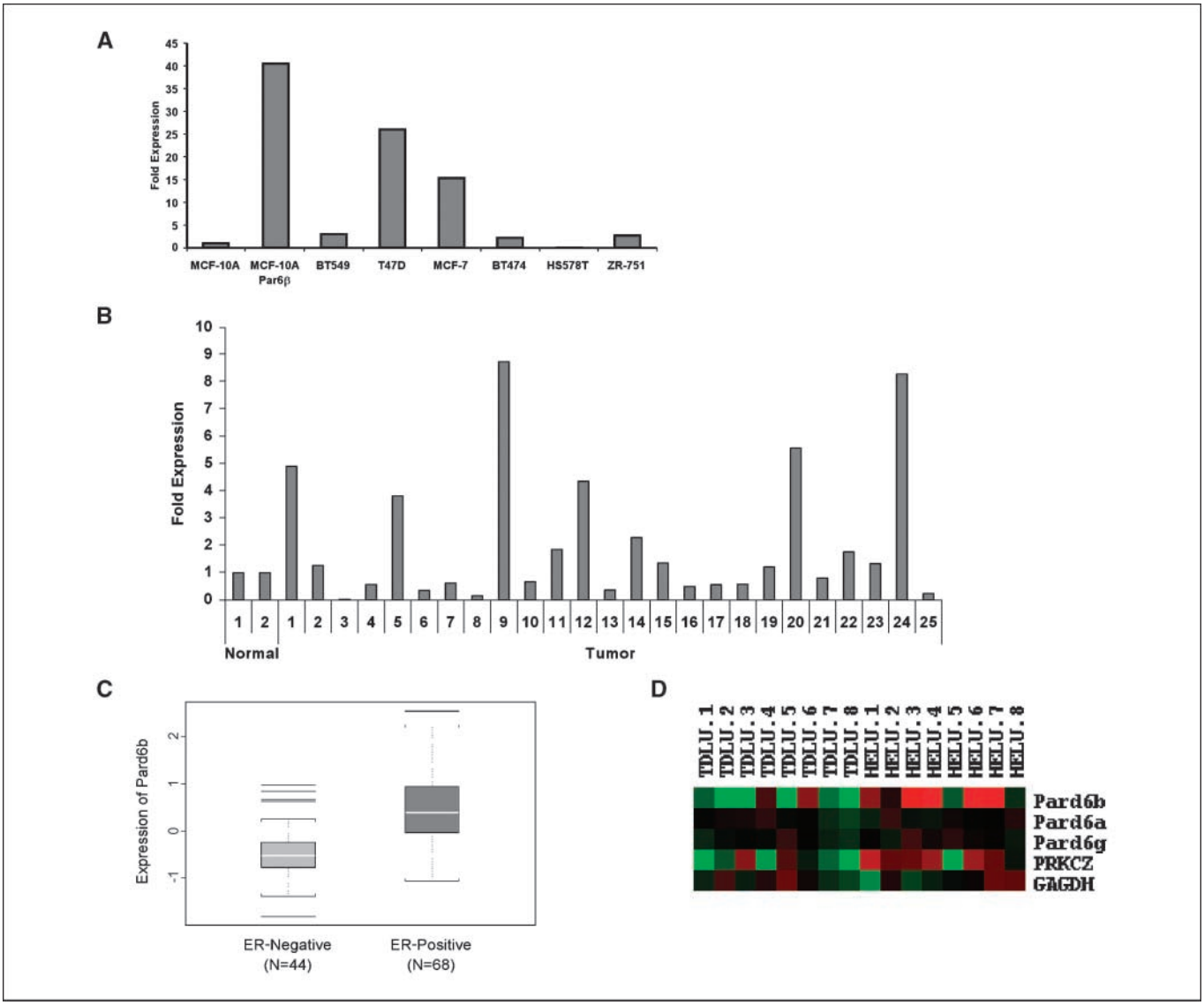

Figure 5. Pard6b is overexpressed in ER-positive human breast tumors. *A,* quantitative PCR analysis of Par6β gene expression using cDNA from breast cancer cell lines and normalized to GAPDH gene expression. Data are represented as fold increase over MCF-10A control cells. *B,* quantitative PCR analysis of Par6β gene expression using cDNA generated from primary breast tumors and normalized to GAPDH gene expression. Data are represented as fold increase over the average levels expressed in normal breast tissue. *C,* a box plot of the microarray data comparing *Pard6b* gene expression in ER^- versus ER^+ tumor samples. A Kolmogorov-Smirnov null hypothesis test was used to calculate the *P* value ($P = 2.9 \times 10^{-7}$). *D,* hierarchical clustering from a supervised comparison between paired samples of normal TDLUs and HELUs. *Pard6b* is expressed 2.5-fold ($P = 0.02$) and *PKCZ* 1.46-fold ($P = 0.029$) in HELU compared with TDLU (45).

cancers. Thus, our results identify a novel role for the polarity protein Par6 as an inducer of cell proliferation, which is likely to play an important role during initiation and progression of breast cancer.

Our results show that overexpression of Par6α and Par6β in nontransformed mammary epithelial cells does not affect establishment of apical-basal polarity during acinar morphogenesis. Whereas several studies have reported that altered expression of both Par6α and Par6β delays establishment of apical polarity (2, 3), they also find that the cells recover from the effects of Par6 overexpression and eventually develop cell polarity. This suggests that compensatory mechanisms act redundantly to ensure apical polarity formation in the presence of altered Par6 expression. Because MCF-10A acinar morphogenesis takes several days, it is likely that Par6-overexpressing cells use these compensatory mechanisms to establish proper apical polarity. We found that ectopic expression of Par6 promotes proliferation of multiple mammary epithelial cell lines, demonstrating that, in addition to its known role as a polarity regulator, Par6 can also induce cell proliferation.

Both aPKC and Cdc42 are required for Par6 to stimulate cell proliferation. This is consistent with the established role of aPKC and Cdc42 in Par6-mediated regulation of tight junction biogenesis, polarized cell migration, and cell death (3, 6, 19, 42). Although previous studies have shown that Par6-induced modulation of GSK3β activity is required for directed cell migration and apoptosis, GSK3β is unlikely to play a role in Par6-induced cell proliferation, because we did not see any differential phosphorylation of GSK3β in Par6-overexpressing cells (data not shown). Instead, we found that Par6 overexpression induces ERK

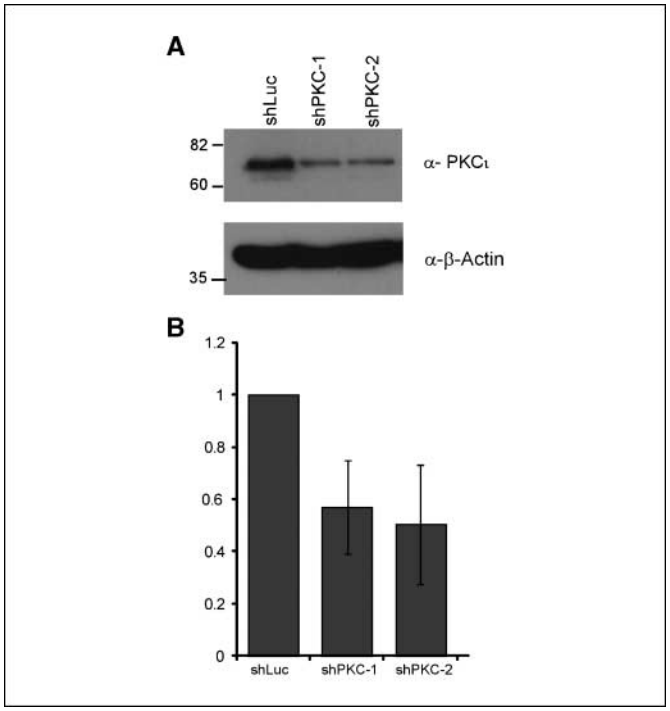

Figure 6. aPKC regulates MCF-7 cell proliferation. *A,* cell extract from PKC short hairpin–infected MCF-10A cells immunoblotted with indicated antibodies. *B,* the indicated cells were grown in growth media containing 10% serum for 7 d, and cell number was determined. Data are fold decrease in cell number of MCF-7shPKC–expressing cells compared with vector control cells. *Columns,* mean of three independent experiments; *bars,* SD.

phosphorylation in the absence of EGF, identifying MAPK pathway as an effector of the Par6-aPKC-Cdc42 complex. MAPK signaling can be activated by ligand-independent phosphorylation of EGFR (43). However, we did not observe phosphorylation of EGFR in the absence of EGF, ruling out a role for EGFR phosphorylation as a mechanism to activate MAPK pathway in Par6-overexpressing cells. Previous studies have shown that PKC is not only sufficient but is also required for activation of ERK in a MEK-dependent manner in response to serum stimulation (44–47). Similarly, we find that Par6 uses aPKC to activate ERK in a MEK-dependent manner. The precise mechanism by which aPKC activates MEK remains to be understood. Thus, in addition to its known effectors that regulate cell polarity, the Par6-aPKC-Cdc42 complex also regulates molecules that induce cell proliferation.

Our results show that Par6β is overexpressed both in HELUs and ER-positive advanced carcinomas. HELUs are characterized by high rates of cell proliferation, ER positivity, and increased expression of EGF family of growth factors. It is possible that HELUs arise from cooperation between overexpressed Par6 and EGF ligands, similar to how Par6 overexpression induced hyperplastic acini in our MCF-10A three-dimensional cultures. Considering that Par6 overexpression promoted hyperplastic acini in MCF-10A three-dimensional culture in cooperation with EGF, it is possible that these two factors could cooperate during development of premalignant lesions in the breast. Our data combined with other studies that show that Par6 is amplified genomically and overexpressed in ER-positive advanced carcinoma suggest that there is a genetic advantage associated with increased Par6 expression during breast cancer progression.

Par6 is also known to cooperate with oncogenes associated with breast cancer progression. For example, Par6 plays a critical role during ErbB2-induced transformation of organized epithelia (20) and ErbB2 amplification is associated with the premalignant breast disease DCIS (48). We did not observe either a positive or negative correlation between Par6 overexpression and ErbB2 status. Therefore, ErbB2 requires expression of Par6, but not overexpression. In addition, Par6 is required for TGFβ-induced epithelial-to-mesenchymal transition, a cellular process that is associated with invasion. The ability of Par6 to interact with oncogenes in distinct cellular processes suggests that Par6 has multiple functions. The results presented in this manuscript, taken together with those above, suggest that the polarity signaling pathways regulated by Par6 plays a cooperative role during the initiation and progression to breast cancer. Thus, a further understanding of the alterations in the Par6 signaling pathways could identify both novel drug targets and predictive biomarkers for breast cancer progression.

Disclosure of Potential Conflicts of Interest

No potential conflicts of interest were disclosed.

Acknowledgments

Received 12/11/2007; revised 6/25/2008; accepted 8/5/2008.

Grant support: U.S. Army predoctoral fellowship grant DAMD 17-03-1-0193 (M.E. Nolan), funding support that include National Cancer Institute grants CA098830 and CA105388 (S.K. Muthuswamy), and grants from Rita Allen Foundation, FACT Foundation, Glen Cove Cares, and Long Islanders Against Breast Cancer.

The costs of publication of this article were defrayed in part by the payment of page charges. This article must therefore be hereby marked *advertisement* in accordance with 18 U.S.C. Section 1734 solely to indicate this fact.

We thank Tony Pawson for Par6a cDNA, Therese Sorlei and Anne Lisa Bornestein for sharing the microarray data, and the members of Muthuswamy laboratory, Daniel Nolan, and Catherine Cormier for helpful suggestions.

References

1. Watts JL, Etemad-Moghadam B, Guo S, et al. par-6, a gene involved in the establishment of asymmetry in early *C. elegans* embryos, mediates the asymmetric localization of PAR-3. Development 1996;122:3133–40.
2. Gao L, Joberty G, Macara IG. Assembly of epithelial tight junctions is negatively regulated by Par6. Curr Biol 2002;12:221–5.
3. Yamanaka T, Horikoshi Y, Suzuki A, et al. PAR-6 regulates aPKC activity in a novel way and mediates cell-cell contact-induced formation of the epithelial junctional complex. Genes Cells 2001;6:721–31.
4. Shi SH, Jan LY, Jan YN. Hippocampal neuronal polarity specified by spatially localized mPar3/mPar6 and PI 3-kinase activity. Cell 2003;112:63–75.
5. Cline EG, Nelson WJ. Characterization of mammalian Par 6 as a dual-location protein. Mol Cell Biol 2007;27:4431–43.
6. Kim M, Datta A, Brakeman P, Yu W, Mostov KE. Polarity proteins PAR6 and aPKC regulate cell death through GSK-3β in 3D epithelial morphogenesis. J Cell Sci 2007;120:2309–17.
7. Etienne-Manneville S, Hall A. Integrin-mediated activation of Cdc42 controls cell polarity in migrating astrocytes through PKCζ. Cell 2001;106:489–98.
8. Kodama A, Karakesisoglou I, Wong E, Vaezi A, Fuchs E. ACF7: an essential integrator of microtubule dynamics. Cell 2003;115:343–54.
9. Solecki DJ, Model L, Gaetz J, Kapoor TM, Hatten ME. Par6α signaling controls glial-guided neuronal migration. Nat Neurosci 2004;7:1195–203.
10. Macara IG. Parsing the polarity code. Nat Rev Mol Cell Biol 2004;5:220–31.
11. Brajenovic M, Joberty G, Kuster B, Bouwmeester T, Drewes G. Comprehensive proteomic analysis of human Par protein complexes reveals an interconnected protein network. J Biol Chem 2004;279:12804–11.

12. Qiu RG, Abo A, Steven Martin G. A human homolog of the *C. elegans* polarity determinant Par-6 links Rac and Cdc42 to PKCζ signaling and cell transformation. Curr Biol 2000;10:697–707.
13. Joberty G, Petersen C, Gao L, Macara IG. The cell-polarity protein Par6 links Par3 and atypical protein kinase C to Cdc42. Nat Cell Biol 2000;2:531–9.
14. Lin D, Edwards AS, Fawcett JP, Mbamalu G, Scott JD, Pawson T. A mammalian PAR-3-PAR-6 complex implicated in Cdc42/Rac1 and aPKC signalling and cell polarity. Nat Cell Biol 2000;2:540–7.
15. Johansson A, Driessens M, Aspenstrom P. The mammalian homologue of the *Caenorhabditis elegans* polarity protein PAR-6 is a binding partner for the Rho GTPases Cdc42 and Rac1. J Cell Sci 2000;113:3267–75.
16. Plant PJ, Fawcett JP, Lin DC, et al. A polarity complex of mPar-6 and atypical PKC binds, phosphorylates and regulates mammalian Lgl. Nat Cell Biol 2003;5:301–8.
17. Suzuki A, Hirata M, Kamimura K, et al. aPKC Acts Upstream of PAR-1b in both the establishment and maintenance of mammalian epithelial polarity. Curr Biol 2004;14:1425–35.
18. Smith CA, Lau KM, Rahmani Z, et al. aPKC-mediated phosphorylation regulates asymmetric membrane localization of the cell fate determinant Numb. EMBO J 2007; 26:468–80.
19. Etienne-Manneville S, Hall A. Cdc42 regulates GSK-3β and adenomatous polyposis coli to control cell polarity. Nature 2003;421:753–6.
20. Aranda V, Haire T, Nolan ME, et al. Par6-aPKC uncouples ErbB2 induced disruption of polarized epithelial organization from proliferation control. Nat Cell Biol 2006;8:1235–45.
21. Ozdamar B, Bose R, Barrios-Rodiles M, Wang HR, Zhang Y, Wrana JL. Regulation of the polarity protein Par6 by TGFβ receptors controls epithelial cell plasticity. Science 2005;307:1603–9.
22. Hicks J, Krasnitz A, Lakshmi B, et al. Novel patterns of genome rearrangement and their association with survival in breast cancer. Genome Res 2006;16:1465–79.
23. Ginestier C, Cervera N, Finetti P, et al. Prognosis and gene expression profiling of 20q13-amplified breast cancers. Clin Cancer Res 2006;12:4533–44.
24. Chin K, DeVries S, Fridlyand J, et al. Genomic and transcriptional aberrations linked to breast cancer pathophysiologies. Cancer Cell 2006;10:529–41.
25. Bergamaschi A, Kim YH, Wang P, et al. Distinct patterns of DNA copy number alteration are associated with different clinicopathological features and gene-expression subtypes of breast cancer. Genes Chromosomes Cancer 2006;45:1033–40.
26. Debnath J, Muthuswamy SK, Brugge JS. Morphogenesis and oncogenesis of MCF-10A mammary epithelial acini grown in three-dimensional basement membrane cultures. Methods 2003;30:256–68.
27. Danielson KG, Oborn CJ, Durban EM, Butel JS, Medina D. Epithelial mouse mammary cell line exhibiting normal morphogenesis *in vivo* and functional differentiation *in vitro*. Proc Natl Acad Sci U S A 1984;81:3756–60.
28. Xian W, Schwertfeger KL, Vargo-Gogola T, Rosen JM. Pleiotropic effects of FGFR1 on cell proliferation, survival, and migration in a 3D mammary epithelial cell model. J Cell Biol 2005;171:663–73.
29. Ory DS, Neugeboren BA, Mulligan RC. A stable human-derived packaging cell line for production of high titer retrovirus/vesicular stomatitis virus G pseudotypes. Proc Natl Acad Sci U S A 1996;93:11400–6.
30. Dickins RA, Hemann MT, Zilfou JT, et al. Probing tumor phenotypes using stable and regulated synthetic microRNA precursors. Nat Genet 2005;37:1289–95.
31. Muthuswamy SK, Li D, Lelievre S, Bissell MJ, Brugge JS. ErbB2, but not ErbB1, reinitiates proliferation and induces luminal repopulation in epithelial acini. Nat Cell Biol 2001;3:785–92.
32. Yamanaka T, Horikoshi Y, Sugiyama Y, et al. Mammalian Lgl forms a protein complex with PAR-6 and aPKC independently of PAR-3 to regulate epithelial cell polarity. Curr Biol 2003;13:734–43.
33. Wilson MI, Gill DJ, Perisic O, Quinn MT, Williams RL. PB1 domain-mediated heterodimerization in NADPH oxidase and signaling complexes of atypical protein kinase C with Par6 and p62. Mol Cell 2003;12:39–50.
34. Wang Q, Hurd TW, Margolis B. Tight junction protein Par6 interacts with an evolutionarily conserved region in the amino terminus of PALS1/stardust. J Biol Chem 2004;279:30715–21.
35. Noda Y, Kohjima M, Izaki T, et al. Molecular recognition in dimerization between PB1 domains. J Biol Chem 2003;278:43516–24.
36. Rhodes DR, Yu J, Shanker K, et al. ONCOMINE: a cancer microarray database and integrated data-mining platform. Neoplasia 2004;6:1–6.
37. Perou CM, Jeffrey SS, van de Rijn M, et al. Distinctive gene expression patterns in human mammary epithelial cells and breast cancers. Proc Natl Acad Sci U S A 1999; 96:9212–7.
38. van de Vijver MJ, He YD, van 't Veer LJ, et al. A gene-expression signature as a predictor of survival in breast cancer. N Engl J Med 2002;347:1999–2009.
39. Zhao H, Langerod A, Ji Y, et al. Different gene expression patterns in invasive lobular and ductal carcinomas of the breast. Mol Biol Cell 2004;15: 2523–36.
40. Lee S, Mohsin SK, Mao S, Hilsenbeck SG, Medina D, Allred DC. Hormones, receptors, and growth in hyperplastic enlarged lobular units: early potential precursors of breast cancer. Breast Cancer Res 2006;8:R6.
41. Lee S, Medina D, Tsimelzon A, et al. Alterations of gene expression in the development of early hyperplastic precursors of breast cancer. Am J Pathol 2007;171:252–62.
42. Gao L, Macara IG, Joberty G. Multiple splice variants of Par3 and of a novel related gene, Par3L, produce proteins with different binding properties. Gene 2002; 294:99–107.
43. Miranti CK, Brugge JS. Sensing the environment: a historical perspective on integrin signal transduction. Nat Cell Biol 2002;4:E83–90.
44. Berra E, Diaz-Meco MT, Dominguez I, et al. Protein kinase C ζ isoform is critical for mitogenic signal transduction. Cell 1993;74:555–63.
45. Berra E, Diaz-Meco MT, Lozano J, et al. Evidence for a role of MEK and MAPK during signal transduction by protein kinase C ζ. EMBO J 1995;14: 6157–63.
46. Bjorkoy G, Perander M, Overvatn A, Johansen T. Reversion of Ras- and phosphatidylcholine-hydrolyzing phospholipase C-mediated transformation of NIH 3T3 cells by a dominant interfering mutant of protein kinase C λ is accompanied by the loss of constitutive nuclear mitogen-activated protein kinase/extracellular signal-regulated kinase activity. J Biol Chem 1997;272:11557–65.
47. Schonwasser DC, Marais RM, Marshall CJ, Parker PJ. Activation of the mitogen-activated protein kinase/extracellular signal-regulated kinase pathway by conventional, novel, and atypical protein kinase C isotypes. Mol Cell Biol 1998;18:790–8.
48. Allred DC, Clark GM, Molina R, et al. Overexpression of HER-2/neu and its relationship with other prognostic factors change during the progression of *in situ* to invasive breast cancer. Hum Pathol 1992;23:974–9.